

1 Title: Innate CD8 $\alpha\alpha^+$ cells and osteopontin promote ILC1-like intraepithelial lymphocyte
2 homeostasis and intestinal inflammation

3

4 Running title: iCD8 α cells and osteopontin promote IEL survival and inflammation

5

6 Authors: Ali Nazmi¹, Kristen Hoek¹, Michael J. Greer², M. Blanca Piazuelo³, Nagahiro Minato⁴
7 and Danyvid Olivares-Villagómez^{1,5,6}

8

9 ¹Department of Pathology, Microbiology and Immunology, Vanderbilt University Medical
10 Center, Nashville, Tennessee, 37232, USA; ²Department of Biomedical Informatics, Vanderbilt
11 University, Nashville, Tennessee, 37232, USA; ³Department of Medicine, Vanderbilt University
12 Medical Center, Nashville, Tennessee, 37232, USA; ⁴Medical Innovation Center, Graduate
13 School of Medicine, Kyoto University, Kyoto 606-8507, Japan; ⁵Vanderbilt Institute for
14 Infection, Immunology and Inflammation, Vanderbilt University Medical Center, Nashville,
15 Tennessee, 37232, USA; ⁶ORCID, 0000-0002-1158-8976.

16

17 Corresponding author: Danyvid Olivares-Villagómez. Telephone, 615-936-0134; fax, 615-343-
18 7392; e-mail, danyvid.olivares-villagomez@vumc.edu

19 Abstract

20 Innate CD8 $\alpha\alpha^+$ cells, also referred to as iCD8 α cells, are TCR-negative intraepithelial
21 lymphocytes (IEL) possessing cytokine and chemokine profiles and functions related to innate
22 immune cells. iCD8 α cells constitute an important source of osteopontin in the intestinal
23 epithelium. Osteopontin is a pleiotropic cytokine with diverse roles in bone and tissue
24 remodeling, but also has relevant functions in the homeostasis of immune cells. In this report, we
25 present evidence for the role of iCD8 α cells and osteopontin in the homeostasis of TCR-negative
26 NKp46 $^+$ NK1.1 $^+$ IEL (ILC1-like). We show that in the absence of iCD8 α cells, the number of
27 NKp46 $^+$ NK1.1 $^+$ IEL is significantly reduced. These ILC1-like cells are involved in intestinal
28 pathogenesis in the anti-CD40 mouse model of intestinal inflammation. Reduced iCD8 α cell
29 numbers and/or osteopontin expression results in a milder form of intestinal inflammation in this
30 disease model. Collectively, our results suggest that iCD8 α cells and osteopontin promote
31 survival of NKp46 $^+$ NK1.1 $^+$ IEL, which significantly impacts the development of intestinal
32 inflammation.

33

34 Introduction

35 Intestinal intraepithelial lymphocytes (IEL) constitute a population of cells dwelling
36 interspersed in the monolayer of intestinal epithelial cells (IEC), and represent a unique
37 immunological compartment in the intestines. Because of their anatomical location, IEL are
38 considered to be the first line of defense against the enormous antigenic stimulus present in the
39 lumen of the intestines. T cell receptor $\alpha\beta^+$ and $\gamma\delta^+$ cells constitute the great majority of IEL [1-
40 3], and these cells possess many and varied roles during mucosal immune responses and
41 inflammatory processes, ranging from specific immunity against pathogens, tissue repair and

42 homeostasis of the intestinal epithelium [4-9]. Lately, it has been recognized that the IEL
43 compartment also harbors TCR^{neg} lymphoid cells with critical roles in mucosal immune
44 responses [3]. The great majority of TCR^{neg} IEL is composed of cells expressing intracellular
45 CD3 γ , which can be divided in CD8 $\alpha\alpha^+$ or CD8 $\alpha\alpha^-$ IEL [10]. TCR^{neg}CD8 $\alpha\alpha^+$ IEL, also referred
46 to as innate CD8 α (iCD8 α) cells, have been previously characterized by our group both in mice
47 and humans [11]. iCD8 α cells possess a chemokine and cytokine signature, antigen processing
48 capabilities, and other functions like bacteria uptake, that suggest that these cells are important
49 during early immune responses [11]. Other TCR^{neg} IEL resemble innate lymphoid cells (ILC)
50 with differential expression of the natural cytotoxicity receptor NKp46 [12-14]. Although their
51 function is not completely understood, NKp46 $^+$ NK1.1 $^+$ IEL have been shown to promote disease
52 development in the anti-CD40 model of colitis [12].

53 The phosphoprotein osteopontin, encoded by the gene Spp-1, is a glycosylated molecule
54 that was originally characterized as part of the rat bone matrix [15, 16], and later shown to
55 induce Th1 responses, promote pathogenic Th17 survival, enhance NKT cell activation of
56 concanavalin A-induced hepatitis, and regulate the homeostasis and function of NK cells [17-
57 21]. A recent publication shows that lack of osteopontin results in reduced TCR $\gamma\delta$ IEL, and that
58 this molecule enhances *in vitro* survival of TCR $\alpha\beta$ and TCR $\gamma\delta$ IEL [22]. In steady state
59 conditions, iCD8 α cells express significant amounts of osteopontin [11], suggesting a potential
60 role for these cells in IEL homeostasis. In terms of intestinal inflammation and disease,
61 osteopontin appears to have divergent roles. For example, in DSS colitis, osteopontin appears to
62 be beneficial during acute disease stages, whereas in chronic disease stages it is detrimental [23].
63 In trinitrobenzene sulphonic acid-induced colitis, osteopontin enhances development of disease
64 [24]. In humans, plasma osteopontin is increased in individuals with inflammatory bowel

65 diseases (IBD) compared to healthy controls [25, 26]. Although a report indicates that
66 osteopontin is downregulated in the mucosa of Crohn's disease patients [27], other groups have
67 reported higher osteopontin expression in the intestines of individuals with ulcerative colitis and
68 Crohn's disease [26, 28]. While these results may be conflicting, they underscore the importance
69 of osteopontin in inflammatory processes and warrant further exploration of this molecule during
70 mucosal immune responses.

71 In this report we investigated the effect of iCD8 α cells as a source of osteopontin in the
72 homeostasis of TCR^{neg} NKp46⁺NK1.1⁺ IEL and their impact in mucosal innate responses. Using
73 mice with reduced iCD8 α cell numbers, we show that these cells have a critical role in
74 NKp46⁺NK1.1⁺ IEL survival, which is in part mediated by osteopontin. Disruption of
75 NKp46⁺NK1.1⁺ IEL homeostasis impacts the development of inflammatory processes in the
76 intestines.

77

78 Materials and methods

79 *Mice.* Rag-2^{-/-} mice in the C57BL/6 background have been in our colony for several years; these

80 mice were originally purchased from the Jackson Laboratories. Spp-1^{-/-} mice in the C57BL/6

81 background were obtained from the Jackson Laboratories. E8_I^{-/-} mice were graciously provided

82 by Dr. Hilde Cheroutre. Spp-1-GFP-Knock-in mice have been previously reported [22]. To

83 homogenize as much as possible the microbiome, all mice obtained from external sources mice

84 were bred in our facility with Rag-2^{-/-} mice to generate heterozygote mice for both mutations,

85 and from these founders we obtained Spp-1^{-/-}Rag-2^{-/-}, E8_I^{-/-}Rag-2^{-/-}, and Rag-2^{-/-}Spp-1-GFP-

86 Knock-in mice. Mice were between 8 to 10-week-old. All mice were bred and housed under

87 similar conditions. The Institutional Animal Care and Use Committee at Vanderbilt University

88 Medical Center approved all animal procedures.

89

90 *IEL isolation.* IEL were isolated by mechanical disruption as previously reported [29]. Briefly,

91 after flushing the intestinal contents with cold HBSS and removing excess mucus, the intestines

92 were cut into small pieces (~1cm long) and shaken for 45 minutes at 37°C in HBSS

93 supplemented with 5% fetal bovine serum and 2mM EDTA. Supernatants were recovered and

94 cells isolated using a discontinuous 40/70% Percoll (General Electric) gradient. In some

95 experiments, IEL preparations were positively enriched using anti-CD45 or anti-CD8_α magnetic

96 beads/columns (Miltenyi).

97

98 *Reagents and flow cytometry.* Fluorochrome-coupled anti-CD8_α, -CD45, -NK1.1, and anti-

99 NKp46 were purchased from Thermo Fisher, BD Biosciences or Tombo. Annexin V and 7AAD

100 were purchased from BD Biosciences. All staining samples were acquired using a FACS Canto

101 II Flow System (BD Biosciences) and data analyzed using FlowJo software (Tree Star). Cell
102 staining was performed following conventional techniques. Manufacturer's instructions were
103 followed for Annexin V staining.

104

105 *In vitro survival assay.* Enriched CD45⁺ IEL (1x10⁵ cells/well) from Rag-2^{-/-} or E8_I^{-/-}Rag-2^{-/-}
106 mice were cultured in a 96-well flat-bottomed well plate in RPMI complemented with 10% fetal
107 bovine serum, penicillin/streptomycin, HEPES, L-glutamine and β-mercaptoethanol in the
108 presence or absence of 2 μg/ml of recombinant osteopontin (R&D) for 4 hours. After incubation,
109 cells were recovered and stained for surface markers, 7AAD and annexin V. In other
110 experiments, enriched CD45⁺ IEL (1x10⁵ cells/well) from Spp-1^{-/-}Rag-2^{-/-} mice were cultured in
111 the presence of enriched iCD8α cells (1x10⁵ cells/well) from Rag-2^{-/-} mice for 4 hours. After
112 incubation, cells were recovered and stained for surface markers, 7AAD and annexin V.

113

114 *Induction of intestinal inflammation with anti-CD40 antibodies.* Eight to ten-week-old female
115 mice over 18g of weight were treated i.p. with 75 or 150μg of anti-mouse CD40 antibody clone
116 FGK4.5 (Bio X Cell) as previously described [30]. Mice were weighted prior to injection and
117 every day thereafter. Mice were monitored daily for signs of disease such as rectal bleeding,
118 diarrhea and scruffiness. At the end point, a portion of the colon was used for pathological
119 examination and scoring as previously reported [30]. All pathological analysis was performed by
120 a GI pathologist (MBP) in a blind fashion. Some mice were treated with recombinant
121 osteopontin (2 μg per mouse i.p.) or PBS at days -2, -1 and 1 pre- and post-disease induction (75
122 μg of anti-CD40).

123

124 *Real-time PCR.* Up to 60 mg of total proximal colon was homogenized using Trizol (Invitrogen)
125 and the RNA was isolated following conventional procedures. RNA was reverse-transcribed
126 using the High Capacity cDNA Transcription Kit (Applied Biosystems). For real-time PCR we
127 used the relative gene expression method [31]. GAPDH served as a normalizer. IL-23p19
128 primers were purchased from QIAGEN and the sequence for osteopontin primers are: Forward:
129 AGCCACAAGTTCACAGCCACAAGG;
130 Reverse: CTGAGAAATGAGCAGTTAGTATTCTGC.

131
132 *Osteopontin protein detection.* For total osteopontin present in tissue, a ~0.5 cm piece of
133 intestine was cultured in a 24-well plate in RPMI containing 10% fetal bovine serum for 24 hrs
134 at 37°C in 5% CO₂. Supernatants were collected and cleared. In another experiment, enriched
135 iCD8α cells were cultured at 1x10⁵ cells/well in a 96-well flat-bottomed plate for 24 hr.
136 Osteopontin concentration was determined in the supernatants using a Quantikine ELISA kit
137 (R&D) following manufacturer's instructions.

138
139 *Statistical analysis.* Statistical significance between the experimental groups was determined by
140 application of an unpaired two-tailed Student's t-test or ANOVA using Prism 7. A *p* value <0.05
141 was considered significant.

142

143 Results

144 *iCD8α cell deficiency results in decreased NKp46⁺NK1.1⁺ IEL*

145 The study of the innate immune system is facilitated by analyzing mice deficient in
146 adaptive immune cells such as Rag-2^{-/-} mice. Analysis of the IEL compartment in these mice
147 showed two main population of cells present in IEL preparations: a population of large cells
148 composed primarily of IEC, and a population of smaller cells constituting lymphoid cells (Fig.
149 1a, left dot plot). The latter population consisted primarily of CD45⁺ cells (Fig. 1a, histogram),
150 which could be divided in CD8αα⁺ and CD8αα^{neg} cells (Fig. 1a right dot plots). The former cells
151 constituted iCD8α cells and represented the majority population of innate cells in the IEL
152 compartment of Rag-2^{-/-} mice. Further subdivision of the CD8αα^{neg} cells showed a well-defined
153 population of NKp46⁺NK1.1⁺ IEL, and other IEL with a gradient expression of NK1.1 (Fig. 1a
154 right dot plots). The E8_I enhancer region is critical for the expression of CD8α homodimers in
155 lymphoid cells present in the intestinal epithelium, without affecting other cells, such as CD8α⁺
156 dendritic cells [32, 33]. In a previous publication, we showed that mice deficient in E8_I present a
157 significant reduction in iCD8α cells [11], and analysis of E8_I^{-/-}Rag-2^{-/-} mice recapitulated this
158 deficiency (Fig. 1a, right dot plots). Because only iCD8α cells express CD8α homodimers, E8_I^{-/-}
159 Rag-2^{-/-} mice serve as a model for iCD8α cell deficiency. Interestingly, E8_I^{-/-}Rag-2^{-/-} mice
160 presented with lower numbers of total CD45⁺ IEL, which may account for the reduction in
161 iCD8α cells (Fig. 1b). Moreover, the IEL compartment of E8_I^{-/-}Rag-2^{-/-} mice also presented a
162 significant reduction in the frequencies and cell numbers of NKp46⁺NK1.1⁺ IEL (Fig. 1b). These
163 cells do not express CD8α homodimers (Fig. 1a, right dot plots) and therefore the decrease in
164 numbers is not directly related with the E8_I mutation.

165

166 *Osteopontin expression in the IEL compartment is primarily associated with iCD8 α cells*

167 Osteopontin is a pleiotropic cytokine that has been reported to sustain homeostasis of lymphoid
168 cells, including NK cells [19] and concanavalin A activated T cells [18]. Because iCD8 α cells
169 have been reported to be a source of osteopontin, we reasoned that the significant absence of
170 these cells in E8 $l^{-/-}$ Rag-2 $^{-/-}$ mice may result in decrease osteopontin production in the intestines.
171 Indeed, the expression of osteopontin mRNA in the intestines of Rag-2 $^{-/-}$ mice was significantly
172 higher than that observed in the intestines of E8 $l^{-/-}$ Rag-2 $^{-/-}$ mice (Fig. 2a). To investigate
173 osteopontin production in the IEL compartment, we analyzed Rag-2 $^{-/-}$ mice carrying the Spp-1-
174 EGFP knock-in reporter gene [22]. Whereas NKp46 $^{+}$ NK1.1 $^{+}$ and other CD8 α^{-} IEL (NKp46 $^{-}$
175 NK1.1 $^{lo/-}$) presented low GFP staining, most iCD8 α cells showed high GFP expression (Fig. 2b),
176 indicating that iCD8 α cells are a key source of osteopontin within innate IEL, and corroborate
177 the reduction of this cytokine in mice deficient in iCD8 α cells (Fig. 2a).

178

179 *iCD8 α cells and osteopontin promote survival of NKp46 $^{+}$ NK1.1 $^{+}$ IEL*

180 The above results suggest that iCD8 α cell-derived osteopontin is important for
181 maintaining normal levels of NKp46 $^{+}$ NK1.1 $^{+}$ cells. One possibility is that osteopontin promotes
182 the survival of these IEL. To test this hypothesis, total enriched-CD45 $^{+}$ IEL from Rag-2 $^{-/-}$ mice
183 were cultured for 4 hours in the presence or absence of recombinant osteopontin, and the survival
184 of NKp46 $^{+}$ NK1.1 $^{+}$ IEL was determined by 7AAD and annexin V staining. As shown in Fig. 3a,
185 recombinant osteopontin did not affect annexin V levels in NKp46 $^{+}$ NK1.1 $^{+}$ IEL derived from
186 Rag-2 $^{-/-}$ mice, suggesting that osteopontin produced by cells present in the culture (like iCD8 α
187 cells, which are the main producers of osteopontin in the intestinal epithelium, Fig. 2b) was
188 sufficient to maintain survival, while addition of exogenous osteopontin did not improve

189 survival. However, when enriched CD45⁺ IEL derived from E8_I^{-/-}Rag-2^{-/-} mice (deficient in
190 iCD8 α cells) were cultured in the presence of recombinant osteopontin, the levels of annexin V
191 staining were lower than in cells cultured in the absence of recombinant osteopontin (Fig. 3b),
192 which suggests that the addition of osteopontin contributes to the survival of NKp46⁺NK1.1⁺
193 IEL from E8_I^{-/-}Rag-2^{-/-} mice. To determine the role of iCD8 α cells in NKp46⁺NK1.1⁺ IEL
194 survival, CD45⁺ IEL from Spp-1^{-/-}Rag-2^{-/-} mice were cultured in the presence or absence of
195 iCD8 α cells from Rag-2^{-/-} mice, which produce osteopontin. As seen in Fig. 3c, addition of
196 iCD8 α cells decreased the level of annexin V staining in NKp46⁺NK1.1⁺ IEL, indicating that
197 iCD8 α cells promote the survival of NKp46⁺NK1.1⁺ IEL.

198 Overall, these results indicate that both, iCD8 α cells and osteopontin, have an important
199 role in the homeostasis of NKp46⁺NK1.1⁺ IEL.

200

201 *Osteopontin kinetics during intestinal inflammation*

202 To investigate the kinetics of osteopontin production during intestinal inflammation, we
203 used the anti-CD40 model of colitis, in which treatment of T and B cell deficient mice (e.g. Rag-
204 2^{-/-}) with anti-CD40 results in weight loss, loose stools, rectal bleeding and inflammation of the
205 colon mediated by IL-23 [30]. This system represents a good model for the analysis of innate
206 immune responses during intestinal inflammation. We treated Rag-2^{-/-} mice with anti-CD40 and
207 2 days after, osteopontin protein levels were measured in colon tissue or enriched-iCD8 α cells.
208 Osteopontin was readily detected either in total colon (Fig. 4a) or iCD8 α cells (Fig. 4b) derived
209 from anti-CD40-treated mice in comparison to naïve animals. To determine the kinetics of
210 osteopontin expression in the intestinal epithelium during inflammation, we treated Rag-2^{-/-}Spp-
211 1-EGFP knock-in reporter mice with anti-CD40. The expression of osteopontin in iCD8 α cells

212 remained constant 3-and 7-days after disease induction, whereas expression of osteopontin in
213 NKp46⁺NK1.1⁺ IEL increased at 3- and 7-days post-treatment (Fig. 4c). On the other hand,
214 expression of osteopontin in other IEL populations (represented as CD8 α ⁻NKp46⁻NK1.1^{lo/-})
215 decreased during the course of the disease (Fig. 4c). These results indicate that during anti-
216 CD40-induced colitis, iCD8 α cells, and to a lesser extent NKp46⁺NK1.1⁺ IEL comprise
217 significant sources of osteopontin in the intestinal epithelium.

218

219 *Osteopontin promotes intestinal inflammation*

220 The increase in osteopontin production observed during anti-CD40-induced colitis
221 suggests an important role for this cytokine in disease development. To test this hypothesis, we
222 treated Rag-2^{-/-} and osteopontin-deficient Rag-2^{-/-} (Spp-1^{-/-}Rag-2^{-/-}) mice with anti-CD40 and
223 monitored the mice for 7 days. As expected, Rag-2^{-/-} mice lost weight starting at day 1 post
224 treatment, which was also observed in Spp-1^{-/-}Rag-2^{-/-} mice (Fig. 5a). However, after day 2, Spp-
225 1^{-/-}Rag-2^{-/-} mice showed significantly decreased weight loss in comparison to Rag-2^{-/-} mice, and
226 presented less colon pathology at the end of the experiment (Fig. 5b). The decrease in disease
227 observed was accompanied by reduced levels of IL-23 expression in the colon (Fig. 5c). These
228 results indicate that osteopontin is detrimental in this model of intestinal inflammation.

229 Interestingly, the numbers of iCD8 α cells and NKp46⁺NK1.1⁺ IEL in naïve Spp-1^{-/-}Rag-
230 2^{-/-} mice were comparable to those observed in Rag-2^{-/-} animals (Fig. 5d), suggesting that the
231 absence of osteopontin has a greater influence in disease development than in the reduction of
232 NKp46⁺NK1.1⁺ IEL numbers.

233

234 *Decreased intestinal inflammation in mice deficient in iCD8a cells*

235 To investigate whether iCD8 α IEL deficiency has an impact in intestinal inflammation, we
236 treated E8 $l^{-/-}$ Rag-2 $^{-/-}$ mice and control Rag-2 $^{-/-}$ mice with anti-CD40. E8 $l^{-/-}$ Rag-2 $^{-/-}$ mice lost less
237 weight throughout the course of the experiment (Fig. 6a) and presented less colon pathology
238 (Fig. 6b), mirroring the observed results in Spp-1 $^{-/-}$ Rag-2 $^{-/-}$ mice (Fig. 5a). Analysis of the
239 kinetics of osteopontin expression in the colon of anti-CD40-treated Rag-2 $^{-/-}$ and E8 $l^{-/-}$ Rag-2 $^{-/-}$
240 mice showed incremental expression of osteopontin mRNA at day 2 and 7 post disease
241 induction; however, the levels of osteopontin mRNA levels were consistently lower in E8 $l^{-/-}$ Rag-
242 2 $^{-/-}$ mice than in Rag-2 $^{-/-}$ mice (Fig. 6c). To investigate whether treatment with osteopontin
243 increases disease severity in iCD8 α cell-deficient mice, E8 $l^{-/-}$ Rag-2 $^{-/-}$ mice were injected i.p. at
244 day -2, -1, and 0 with recombinant osteopontin, followed by disease induction with a reduced
245 dose of anti-CD40 at day 0 (a lower dose was chosen to better detect changes in disease
246 severity). Rag-2 $^{-/-}$ control mice lost similar weight with low anti-CD40 than mice treated with the
247 regular dose (compare Fig. 6a and 6d); however, E8 $l^{-/-}$ Rag-2 $^{-/-}$ mice treated with low anti-CD40
248 recovered faster than E8 $l^{-/-}$ Rag-2 $^{-/-}$ mice treated with the full anti-CD40 dose (compare Fig. 6a
249 and 6d). Although, E8 $l^{-/-}$ Rag-2 $^{-/-}$ mice treated with recombinant osteopontin presented weight
250 loss similar to PBS-treated E8 $l^{-/-}$ Rag-2 $^{-/-}$ mice during the first few days after disease induction,
251 the former group did not recover as the PBS-treated group and their weights were more similar to
252 Rag-2 $^{-/-}$ control mice. (Fig. 6d). Although colon pathological scores were comparable between
253 the control and recombinant osteopontin-treated E8 $l^{-/-}$ Rag-2 $^{-/-}$ groups, there was a tendency for
254 higher disease severity in the latter group. Therefore, our results indicate that administration of
255 osteopontin slightly increases disease severity in the absence of iCD8 α cells and low osteopontin
256 expression in the colon.

257

258 Discussion

259 Osteopontin is known to be widely expressed in the intestinal mucosa of ulcerative colitis and
260 Crohn's disease patients, and in the latter group, osteopontin plasma levels are increased in
261 comparison to control individuals [26, 34], suggesting an involvement of this molecule in the
262 pathology of inflammatory bowel diseases. However, the role of osteopontin in mouse models of
263 intestinal inflammation is controversial. In the DSS model of colitis, reports vary about the role
264 of osteopontin, either as a pro or anti-inflammatory factor [23, 34-36]. Moreover, in the
265 trinitrobenzene sulphonic acid-induced model of colitis, osteopontin-deficient mice fare better
266 than wild type animals, suggesting a pro-inflammatory role for this cytokine [37]. In contrast, in
267 the IL-10-deficiency model of spontaneous intestinal inflammation, IL-10^{-/-}Spp-1^{-/-} mice develop
268 disease faster than IL-10^{-/-} control mice [36]. Finally, adoptive transfer of naïve CD62L^{hi}CD4⁺ T
269 cells into Rag-2^{-/-}Spp-1^{-/-} mice resulted in less chronic colitis than Rag-2^{-/-} recipient mice [38].
270 How to reconcile these diverse observations? It is possible that osteopontin's impact varies
271 depending on the primary cell populations responsible for disease induction or the disease stage.
272 For example, here we propose that iCD8 α cells, via osteopontin, promote the survival of pro-
273 inflammatory NKp46⁺NK1.1⁺ IEL during acute colitis, whereas in other disease models
274 osteopontin may differentially impact acute and chronic inflammation [23]. Therefore, dissecting
275 how osteopontin affects different branches of the mucosal immune system during steady state
276 levels and inflammatory processes is of critical relevance to increase our understanding of IEL
277 biology and osteopontin function, as well as the impact of this cytokine in diseases such as
278 ulcerative colitis and Crohn's disease.

279 IEL reside in a unique anatomical location intercalated between IEC, and in close
280 proximity to the contents of the intestinal lumen. This location makes a unique niche for IEL. In

281 this environment, IEL are most likely subjected to distinctive signals during steady-state levels as
282 well as during intestinal immune responses. In addition, IEL represent a heterogeneous
283 population of lymphocytes with different developmental origins and immunological roles [1-3],
284 and because of this diversity, each IEL population may be subjected to particular environmental
285 clues. How different IEL populations survive and maintain homeostasis in the intestinal
286 epithelium is not very well understood. In this report, we examine the role of a novel IEL
287 population referred to as iCD8 α cells and the pleiotropic cytokine osteopontin in the homeostasis
288 of NKp46 $^+$ NK1.1 $^+$ IEL. iCD8 α cells promote clearance of the colitis-inducing pathogen
289 *Citrobacter rodentium* [11], but also exacerbate colitis via granzymes when not properly
290 regulated [39]. The results presented in this report add a new role for iCD8 α IEL as a population
291 promoting the survival of NKp46 $^+$ NK1.1 $^+$ IEL via osteopontin.

292 Although most of the IEL studies have primarily focused on TCR $^+$ IEL (TCR $\alpha\beta$ and $\gamma\delta$),
293 recently it has become apparent that TCR $^{\text{neg}}$ IEL constitute an important fraction of the IEL
294 compartment. Three distinct TCR $^{\text{neg}}$ IEL populations have been characterized to date: iCD3 $^+$,
295 iCD8 α , and ILC-like IEL [10, 12-14]. iCD3 $^+$ and iCD8 α cells appear to be related IEL
296 populations that require IL-15 for their development. How the homeostasis of these cells is
297 maintained in the intestinal epithelium is not clearly understood. There is evidence suggesting
298 that the thymus leukemia (TL) antigen, a ligand for CD8 $\alpha\alpha$ homodimers [40, 41], is needed for
299 maintenance of iCD8 α cells [11]. Some ILC-like IEL require IL-15 for their survival, such as
300 NKp46-negative IEL [14]. Although osteopontin deficient mice present similar numbers of
301 NKp46 $^+$ NK1.1 $^+$ IEL (Fig. 5d), their numbers are significantly decreased in mice deficient in
302 iCD8 α cells and reduced intestinal osteopontin (E8 $^{-/-}$ Rag-2 $^{-/-}$ mice). These observations raise the

303 possibility that iCD8 α cells support NKp46 $^+$ NK1.1 $^+$ IEL homeostasis by unknown mechanisms
304 in addition to osteopontin.

305 Our *in vivo* evidence presented in this report indicates that iCD8 α cells represent one of
306 the innate IEL populations with highest levels of osteopontin expression, and that mice deficient
307 in iCD8 α cells also present decreased osteopontin levels in the colon (Fig. 2a). These results
308 suggest a putative role for iCD8 α cells as a source of osteopontin in the intestinal epithelium,
309 allowing proper survival of other IEL in steady state conditions. Although NKp46 $^+$ NK1.1 $^+$ IEL
310 do not produce osteopontin during steady state conditions, the expression of this cytokine
311 incrementally appears at day 3 and 7 post anti-CD40 treatment. At this moment, the significance
312 of NKp46 $^+$ NK1.1 $^+$ IEL-derived osteopontin during inflammation is unknown.

313 It is important to mention that in order to study innate IEL, our results are based on mice
314 lacking TCR $^+$ IEL, and therefore, we do not discard the possibility that some TCR $^+$ IEL may be
315 osteopontin producers in wild type mice. Indeed, in steady state conditions, using an osteopontin-
316 GFP reporter system, Hattori's group showed that TCR $^+$ CD8 α $^+$ IEL represent a source of
317 osteopontin in the intestines of wild type mice [22]. This group also showed that TCR $\gamma\delta$ $^+$ IEL *in*
318 *vivo* are dependent on osteopontin for their survival, whereas in *in vitro* conditions, both
319 TCR $\alpha\beta$ $^+$ and $\gamma\delta$ $^+$ IEL survival is blunted by anti-osteopontin antibodies. Although, the report by
320 Hattori's group and our results presented herein clearly indicate an important role for osteopontin
321 in IEL survival, there is still a significant gap in knowledge about the homeostasis of IEL
322 subpopulations, such as TCR β $^+$ CD4 $^+$, TCR β $^+$ CD4 $^+$ CD8 $\alpha\alpha$ $^+$, TCR β $^+$ CD8 $\alpha\beta$ $^+$, TCR β $^+$ CD8 $\alpha\alpha$ $^+$
323 and CD8 $\alpha\alpha$ neg CD3 $^+$ cells; similarly, it is unknown whether human IEL require osteopontin for
324 their survival/homeostasis. Another outstanding question is the receptor used by osteopontin to

325 stimulate IEL. One possible candidate is CD44, a molecule expressed in activated T cells, with
326 the capacity of binding osteopontin [42].

327 It is poorly investigated whether different population of IEL interact with each other.

328 There are few reports that indirectly suggest that this could be the case, for example, TCR $\gamma\delta$ IEL
329 control the activation status and numbers of TCR $\alpha\beta^+$ CD8 $\alpha\beta^+$ IEL in humans [43], whereas
330 iCD8 α cells may present antigen to CD4 $^+$ IEL in an MHC class II restricted fashion [11].

331 Although our results do not provide direct evidence showing interaction between iCD8 α cells
332 and NKp46 $^+$ NK1.1 $^+$ IEL in the intestinal epithelium, IEL may either directly interact with each
333 other or may communicate via cytokines and/or other factors. However, more research needs to
334 be done to have a better understanding of IEL-IEL interactions.

335 In conclusion, in this report we provide evidence indicating an important and novel role
336 for iCD8 α cells in the homeostasis of NKp46 $^+$ NK1.1 $^+$ IEL. We also show that the effect of
337 iCD8 α cells is mediated in part by osteopontin, which adds to the growing roles of this cytokine
338 in different biological processes.

339

340 Acknowledgements: We thank the Translational Pathology Shared Resource for tissue
341 processing. This work was supported by NIH grant R01DK111671 (to D.O-V.); Careers in
342 Immunology Fellowship Program from the American Association of Immunologist (to D.O-V.
343 and A.N.); National Library of Medicine T15 LM00745 grant (to M.J.G.); and scholarships from
344 the Digestive Disease Research Center at Vanderbilt University Medical Center supported by
345 NIH grant P30DK058404.

346

347

348 References

349 1. Van Kaer L, Olivares-Villagomez D. Development, Homeostasis, and Functions of
350 Intestinal Intraepithelial Lymphocytes. *J Immunol.* 2018;200(7):2235-44. Epub 2018/03/21. doi:
351 10.4049/jimmunol.1701704. PubMed PMID: 29555677; PubMed Central PMCID:
352 PMCPMC5863587.

353 2. Cheroutre H. Starting at the beginning: new perspectives on the biology of mucosal T
354 cells. *Annu Rev Immunol.* 2004;22:217-46. PubMed PMID: 15032579.

355 3. Olivares-Villagomez D, Van Kaer L. Intestinal Intraepithelial Lymphocytes: Sentinels of
356 the Mucosal Barrier. *Trends Immunol.* 2017. Epub 2017/12/10. doi: 10.1016/j.it.2017.11.003.
357 PubMed PMID: 29221933.

358 4. Chen Y, Chou K, Fuchs E, Havran WL, Boismenu R. Protection of the intestinal mucosa
359 by intraepithelial gamma delta T cells. *Proc Natl Acad Sci U S A.* 2002;99(22):14338-43.
360 PubMed PMID: 12376619.

361 5. Das G, Augustine MM, Das J, Bottomly K, Ray P, Ray A. An important regulatory role
362 for CD4+CD8 alpha alpha T cells in the intestinal epithelial layer in the prevention of
363 inflammatory bowel disease. *Proc Natl Acad Sci U S A.* 2003;100(9):5324-9. PMC1535703.
364 PubMed PMID: 12695566.

365 6. Guy-Grand D, DiSanto JP, Henchoz P, Malassis-Seris M, Vassalli P. Small bowel
366 enteropathy: role of intraepithelial lymphocytes and of cytokines (IL-12, IFN-gamma, TNF) in
367 the induction of epithelial cell death and renewal. *Eur J Immunol.* 1998;28(2):730-44. PubMed
368 PMID: 9521083.

369 7. Inagaki-Ohara K, Chinen T, Matsuzaki G, Sasaki A, Sakamoto Y, Hiromatsu K, et al.

370 Mucosal T cells bearing TCRgammadelta play a protective role in intestinal inflammation. *J*

371 *Immunol.* 2004;173(2):1390-8. PubMed PMID: 15240735.

372 8. Lepage AC, Buzoni-Gatel D, Bout DT, Kasper LH. Gut-derived intraepithelial

373 lymphocytes induce long term immunity against *Toxoplasma gondii*. *J Immunol.*

374 1998;161(9):4902-8. PubMed PMID: 9794424.

375 9. Masopust D, Jiang J, Shen H, Lefrancois L. Direct analysis of the dynamics of the

376 intestinal mucosa CD8 T cell response to systemic virus infection. *J Immunol.*

377 2001;166(4):2348-56. PubMed PMID: 11160292.

378 10. Ettersperger J, Montcuquet N, Malamut G, Guegan N, Lopez-Lastra S, Gayraud S, et al.

379 Interleukin-15-Dependent T-Cell-like Innate Intraepithelial Lymphocytes Develop in the

380 Intestine and Transform into Lymphomas in Celiac Disease. *Immunity.* 2016;45(3):610-25. Epub

381 2016/09/11. doi: 10.1016/j.jimmuni.2016.07.018. PubMed PMID: 27612641.

382 11. Van Kaer L, Algood HM, Singh K, Parekh VV, Greer MJ, Piazuelo MB, et al.

383 CD8alphaalpha(+) Innate-Type Lymphocytes in the Intestinal Epithelium Mediate Mucosal

384 Immunity. *Immunity.* 2014;41(3):451-64. Epub 2014/09/16. doi: 10.1016/j.jimmuni.2014.08.010.

385 PubMed PMID: 25220211; PubMed Central PMCID: PMC4169715.

386 12. Fuchs A, Vermi W, Lee JS, Lonardi S, Gilfillan S, Newberry RD, et al. Intraepithelial

387 type 1 innate lymphoid cells are a unique subset of IL-12- and IL-15-responsive IFN-gamma-

388 producing cells. *Immunity.* 2013;38(4):769-81. Epub 2013/03/05. doi:

389 10.1016/j.jimmuni.2013.02.010. PubMed PMID: 23453631; PubMed Central PMCID:

390 PMC3634355.

391 13. Talayero P, Mancebo E, Calvo-Pulido J, Rodriguez-Munoz S, Bernardo I, Laguna-Goya
392 R, et al. Innate Lymphoid Cells Groups 1 and 3 in the Epithelial Compartment of Functional
393 Human Intestinal Allografts. *Am J Transplant.* 2016;16(1):72-82. Epub 2015/09/01. doi:
394 10.1111/ajt.13435. PubMed PMID: 26317573.

395 14. Van Acker A, Gronke K, Biswas A, Martens L, Saeys Y, Filtjens J, et al. A Murine
396 Intestinal Intraepithelial NKp46-Negative Innate Lymphoid Cell Population Characterized by
397 Group 1 Properties. *Cell Rep.* 2017;19(7):1431-43. doi: 10.1016/j.celrep.2017.04.068. PubMed
398 PMID: 28514662.

399 15. Franzen A, Heinegard D. Isolation and characterization of two sialoproteins present only
400 in bone calcified matrix. *Biochem J.* 1985;232(3):715-24. Epub 1985/12/15. PubMed PMID:
401 4091817; PubMed Central PMCID: PMCPMC1152943.

402 16. Prince CW, Oosawa T, Butler WT, Tomana M, Bhow AS, Bhow M, et al. Isolation,
403 characterization, and biosynthesis of a phosphorylated glycoprotein from rat bone. *J Biol Chem.*
404 1987;262(6):2900-7. Epub 1987/02/25. PubMed PMID: 3469201.

405 17. Ashkar S, Weber GF, Panoutsakopoulou V, Sanchirico ME, Jansson M, Zawaideh S, et
406 al. Eta-1 (osteopontin): an early component of type-1 (cell-mediated) immunity. *Science.*
407 2000;287(5454):860-4. Epub 2000/02/05. PubMed PMID: 10657301.

408 18. Hur EM, Youssef S, Haws ME, Zhang SY, Sobel RA, Steinman L. Osteopontin-induced
409 relapse and progression of autoimmune brain disease through enhanced survival of activated T
410 cells. *Nat Immunol.* 2007;8(1):74-83. Epub 2006/12/05. doi: 10.1038/ni1415. PubMed PMID:
411 17143274.

412 19. Leavenworth JW, Verbinnen B, Wang Q, Shen E, Cantor H. Intracellular osteopontin
413 regulates homeostasis and function of natural killer cells. *Proc Natl Acad Sci U S A.*

414 2015;112(2):494-9. Epub 2015/01/01. doi: 10.1073/pnas.1423011112. PubMed PMID:
415 25550515; PubMed Central PMCID: PMC4299239.

416 20. Murugaiyan G, Mittal A, Weiner HL. Increased osteopontin expression in dendritic cells
417 amplifies IL-17 production by CD4+ T cells in experimental autoimmune encephalomyelitis and
418 in multiple sclerosis. *J Immunol.* 2008;181(11):7480-8. Epub 2008/11/20. PubMed PMID:
419 19017937; PubMed Central PMCID: PMC2653058.

420 21. Staines KA, MacRae VE, Farquharson C. The importance of the SIBLING family of
421 proteins on skeletal mineralisation and bone remodelling. *The Journal of endocrinology.*
422 2012;214(3):241-55. Epub 2012/06/16. doi: 10.1530/JOE-12-0143. PubMed PMID: 22700194.

423 22. Ito K, Nakajima A, Fukushima Y, Suzuki K, Sakamoto K, Hamazaki Y, et al. The
424 potential role of Osteopontin in the maintenance of commensal bacteria homeostasis in the
425 intestine. *PLoS One.* 2017;12(3):e0173629. Epub 2017/03/16. doi:
426 10.1371/journal.pone.0173629. PubMed PMID: 28296922; PubMed Central PMCID:
427 PMCPMC5351998.

428 23. Heilmann K, Hoffmann U, Witte E, Loddenkemper C, Sina C, Schreiber S, et al.
429 Osteopontin as two-sided mediator of intestinal inflammation. *Journal of cellular and molecular*
430 *medicine.* 2009;13(6):1162-74. Epub 2008/07/17. doi: 10.1111/j.1582-4934.2008.00428.x.
431 PubMed PMID: 18627421; PubMed Central PMCID: PMC4496111.

432 24. Oz HS, Zhong J, de Villiers WJ. Osteopontin ablation attenuates progression of colitis in
433 TNBS model. *Dig Dis Sci.* 2012;57(6):1554-61. Epub 2011/12/17. doi: 10.1007/s10620-011-
434 2009-z. PubMed PMID: 22173746.

435 25. Mishima R, Takeshima F, Sawai T, Ohba K, Ohnita K, Isomoto H, et al. High plasma
436 osteopontin levels in patients with inflammatory bowel disease. *J Clin Gastroenterol.*

437 2007;41(2):167-72. Epub 2007/01/25. doi: 10.1097/MCG.0b013e31802d6268. PubMed PMID:
438 17245215.

439 26. Sato T, Nakai T, Tamura N, Okamoto S, Matsuoka K, Sakuraba A, et al.

440 Osteopontin/Eta-1 upregulated in Crohn's disease regulates the Th1 immune response. Gut.
441 2005;54(9):1254-62. Epub 2005/08/16. doi: 10.1136/gut.2004.048298. PubMed PMID:
442 16099792; PubMed Central PMCID: PMC1774642.

443 27. Gassler N, Autschbach F, Gauer S, Bohn J, Sido B, Otto HF, et al. Expression of
444 osteopontin (Eta-1) in Crohn disease of the terminal ileum. Scand J Gastroenterol.
445 2002;37(11):1286-95. Epub 2002/12/06. PubMed PMID: 12465727.

446 28. Masuda H, Takahashi Y, Asai S, Takayama T. Distinct gene expression of osteopontin in
447 patients with ulcerative colitis. J Surg Res. 2003;111(1):85-90. Epub 2003/07/05. PubMed
448 PMID: 12842452.

449 29. Olivares-Villagomez D, Mendez-Fernandez YV, Parekh VV, Lalani S, Vincent TL,
450 Cheroutre H, et al. Thymus leukemia antigen controls intraepithelial lymphocyte function and
451 inflammatory bowel disease. Proc Natl Acad Sci U S A. 2008;105(46):17931-6. PMC2584730.
452 PubMed PMID: 19004778.

453 30. Uhlig HH, McKenzie BS, Hue S, Thompson C, Joyce-Shaikh B, Stepankova R, et al.
454 Differential activity of IL-12 and IL-23 in mucosal and systemic innate immune pathology.
455 Immunity. 2006;25(2):309-18. Epub 2006/08/22. doi: 10.1016/j.immuni.2006.05.017. PubMed
456 PMID: 16919486.

457 31. Giulietti A, Overbergh L, Valckx D, Decallonne B, Bouillon R, Mathieu C. An overview
458 of real-time quantitative PCR: applications to quantify cytokine gene expression. Methods.

459 2001;25(4):386-401. Epub 2002/02/16. doi: 10.1006/meth.2001.1261. PubMed PMID: 11846608.

460

461 32. Ellmeier W, Sawada S, Littman DR. The regulation of CD4 and CD8 coreceptor gene

462 expression during T cell development. *Annu Rev Immunol.* 1999;17:523-54. Epub 1999/06/08.

463 doi: 10.1146/annurev.immunol.17.1.523. PubMed PMID: 10358767.

464 33. Taniuchi I, Ellmeier W, Littman DR. The CD4/CD8 lineage choice: new insights into

465 epigenetic regulation during T cell development. *Advances in immunology.* 2004;83:55-89.

466 Epub 2004/05/12. doi: 10.1016/S0065-2776(04)83002-5. PubMed PMID: 15135628.

467 34. Masuda H, Takahashi Y, Asai S, Hemmi A, Takayama T. Osteopontin expression in

468 ulcerative colitis is distinctly different from that in Crohn's disease and diverticulitis. *J*

469 *Gastroenterol.* 2005;40(4):409-13. Epub 2005/05/04. doi: 10.1007/s00535-005-1567-2. PubMed

470 PMID: 15868372.

471 35. Zhong J, Eckhardt ER, Oz HS, Bruemmer D, de Villiers WJ. Osteopontin deficiency

472 protects mice from Dextran sodium sulfate-induced colitis. *Inflamm Bowel Dis.* 2006;12(8):790-

473 6. Epub 2006/08/19. PubMed PMID: 16917234.

474 36. Toyonaga T, Nakase H, Ueno S, Matsuura M, Yoshino T, Honzawa Y, et al. Osteopontin

475 Deficiency Accelerates Spontaneous Colitis in Mice with Disrupted Gut Microbiota and

476 Macrophage Phagocytic Activity. *PLoS One.* 2015;10(8):e0135552. Epub 2015/08/15. doi:

477 10.1371/journal.pone.0135552. PubMed PMID: 26274807; PubMed Central PMCID:

478 PMC4537118.

479 37. Kourepini E, Aggelakopoulou M, Alissafi T, Paschalidis N, Simoes DC,

480 Panoutsakopoulou V. Osteopontin expression by CD103- dendritic cells drives intestinal

481 inflammation. *Proc Natl Acad Sci U S A.* 2014;111(9):E856-65. Epub 2014/02/20. doi:
482 10.1073/pnas.1316447111. PubMed PMID: 24550510; PubMed Central PMCID: PMC3948306.

483 38. Kanayama M, Xu S, Danzaki K, Gibson JR, Inoue M, Gregory SG, et al. Skewing of the
484 population balance of lymphoid and myeloid cells by secreted and intracellular osteopontin. *Nat*
485 *Immunol.* 2017;18(9):973-84. Epub 2017/07/04. doi: 10.1038/ni.3791. PubMed PMID:
486 28671690; PubMed Central PMCID: PMCPMC5568448.

487 39. Kumar AA, Delgado AG, Piazuelo MB, Van Kaer L, Olivares-Villagomez D. Innate
488 CD8alphaalpha+ lymphocytes enhance anti-CD40 antibody-mediated colitis in mice. *Immun*
489 *Inflamm Dis.* 2017;5(2):109-23. doi: 10.1002/iid3.146. PubMed PMID: 28474503; PubMed
490 Central PMCID: PMCPMC5418141.

491 40. Leishman AJ, Naidenko OV, Attinger A, Koning F, Lena CJ, Xiong Y, et al. T cell
492 responses modulated through interaction between CD8alphaalpha and the nonclassical MHC
493 class I molecule, TL. *Science.* 2001;294(5548):1936-9. PubMed PMID: 11729321.

494 41. Teitell M, Mescher MF, Olson CA, Littman DR, Kronenberg M. The thymus leukemia
495 antigen binds human and mouse CD8. *J Exp Med.* 1991;174(5):1131-8. PubMed PMID:
496 1834760.

497 42. Weber GF, Ashkar S, Glimcher MJ, Cantor H. Receptor-ligand interaction between
498 CD44 and osteopontin (Eta-1). *Science.* 1996;271(5248):509-12. Epub 1996/01/26. PubMed
499 PMID: 8560266.

500 43. Bhagat G, Naiyer AJ, Shah JG, Harper J, Jabri B, Wang TC, et al. Small intestinal
501 CD8+TCRgammadelta+NKG2A+ intraepithelial lymphocytes have attributes of regulatory cells
502 in patients with celiac disease. *J Clin Invest.* 2008;118(1):281-93. Epub 2007/12/08. doi:
503 10.1172/JCI30989. PubMed PMID: 18064301; PubMed Central PMCID: PMCPMC2117760.

504 Figure legends

505 Fig. 1. *iCD8α cell deficiency results in decreased NKp46⁺NK1.1⁺IEL numbers*. Total IEL from
506 Rag-2^{-/-} and E8_I^{-/-}Rag-2^{-/-} mice were analyzed for the presence of CD45⁺ and CD45⁺CD8α⁻
507 NKp46⁺NK1.1⁺ IEL. (a) Gating strategy for the analysis of the IEL compartment used
508 throughout this report. Dead cells were excluded using a viability dye. (b) Total IEL numbers of
509 the indicated subpopulations. Each symbol represents an individual mouse (n=7 to 8). Data are
510 representative of at least two independent experiments. *p<0.05, ***p<0.001 using unpaired
511 two-tailed Student's T test.

512

513 Fig. 2. *Osteopontin expression in the IEL compartment is primarily associated with iCD8α cells*.
514 (a) Osteopontin mRNA expression in colon of the indicated mice. Expression levels in E8_I^{-/-}Rag-
515 2^{-/-} mice were compared to the average expression levels observed in Rag-2^{-/-} mice. Each symbol
516 represents an individual mouse (n=7 to 8). Data are the combination of two independent
517 experiments. (b) Osteopontin expression in naïve Rag-2^{-/-}Spp-1-EGFP-KI mice. Histogram is a
518 representative mouse (n=4). Data are representative of at least two independent experiments.
519 **p<0.01, using unpaired two-tailed Student's T test for (a) and non-parametric one-way
520 ANOVA for (b).

521

522 Fig. 3. *iCD8α cells and osteopontin promote survival of NKp46⁺NK1.1⁺ IEL*. Enriched CD45⁺
523 IEL from Rag-2^{-/-} (a) or E8_I^{-/-}Rag-2^{-/-} (b) mice were incubated in the presence or absence of
524 recombinant osteopontin (2μg/ml final concentration). Cells were recovered 4 hours later and
525 analyzed for annexin V staining on NKp46⁺NK1.1⁺ IEL as indicated in the Materials and
526 methods section. Data are representative of at least two independent experiments (n=4). (c)

527 Enriched CD45⁺ cells from Spp-1^{-/-}Rag-2^{-/-} mice were incubated in the presence or absence of
528 iCD8 α cells derived from Rag-2^{-/-} mice. Cells were recovered 4 hours later and analyzed for
529 annexin V staining on NKp46⁺NK1.1⁺ IEL as indicated in the Materials and Method section. In
530 order to obtain enough iCD8 α cells, 2-3 mice were pooled and counted as one sample (n=4).
531 Data is representative of at least 2 experiments. * $p<0.05$, using unpaired two-tailed Student's T
532 test.

533

534 Fig. 4. *Osteopontin kinetics during intestinal inflammation.* (a) Osteopontin protein
535 concentration in the supernatants of whole colon tissue cultures from naïve and anti-CD40-
536 treated Rag-2^{-/-} mice. Data is representative of at least 2 experiments (n=5). (b) Osteopontin
537 protein concentration in the supernatants of iCD8 α cells derived from naïve and anti-CD40-
538 treated Rag-2^{-/-} mice. Data is representative of at least two experiments. In order to obtain
539 enough iCD8 α cells, 2-3 mice were pooled and counted as one sample (n=3). (c) GFP expression
540 in Rag-2^{-/-}Spp-1-EGFP-KI mice treated with anti-CD40 and analyzed at the indicated time
541 points. Cells were gated as indicated in Fig.1a. Histograms are from a representative sample. Bar
542 graph shows data summary. * $p<0.05$, *** $p<0.001$ using unpaired two-tailed Student's T test.

543

544 Fig. 5. *Osteopontin promotes intestinal inflammation.* (a) Rag-2^{-/-} and Spp-1^{-/-}Rag-2^{-/-} mice were
545 treated with 150 μ g of anti-CD40 and monitored daily for weight change for 7 days. (b)
546 Pathological representation (micrographs, magnification 200X) and disease score; each symbol
547 represents an individual mouse (n=5 to 6). Data is representative of at least 2 experiments. (c) IL-
548 23p19 mRNA expression from total colons; each symbol represents an individual mouse (n=5 to
549 6). Data is representative of at least 2 experiments. (d) Total iCD8 α cell and NKp46⁺NK1.1⁺ IEL

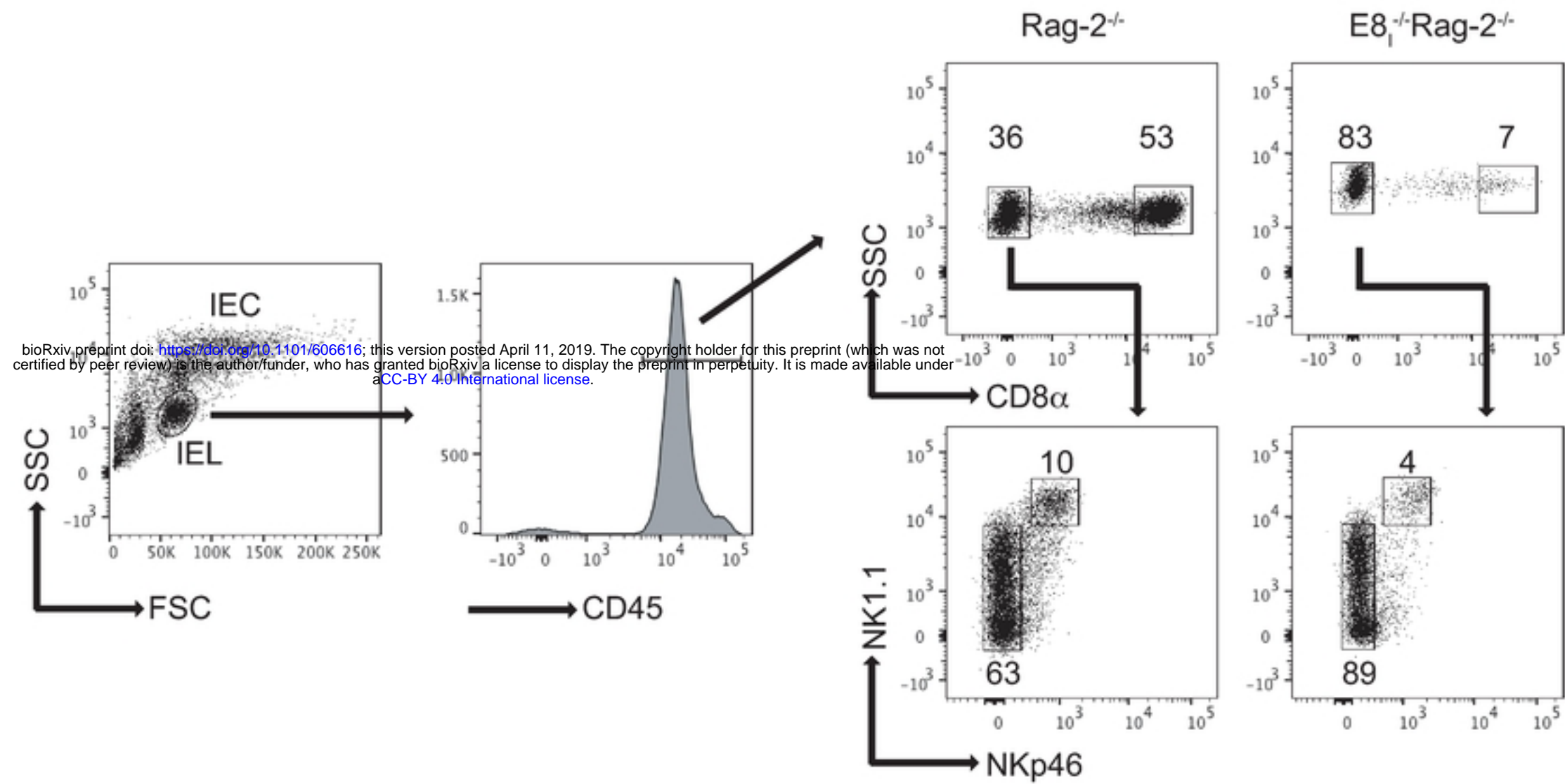
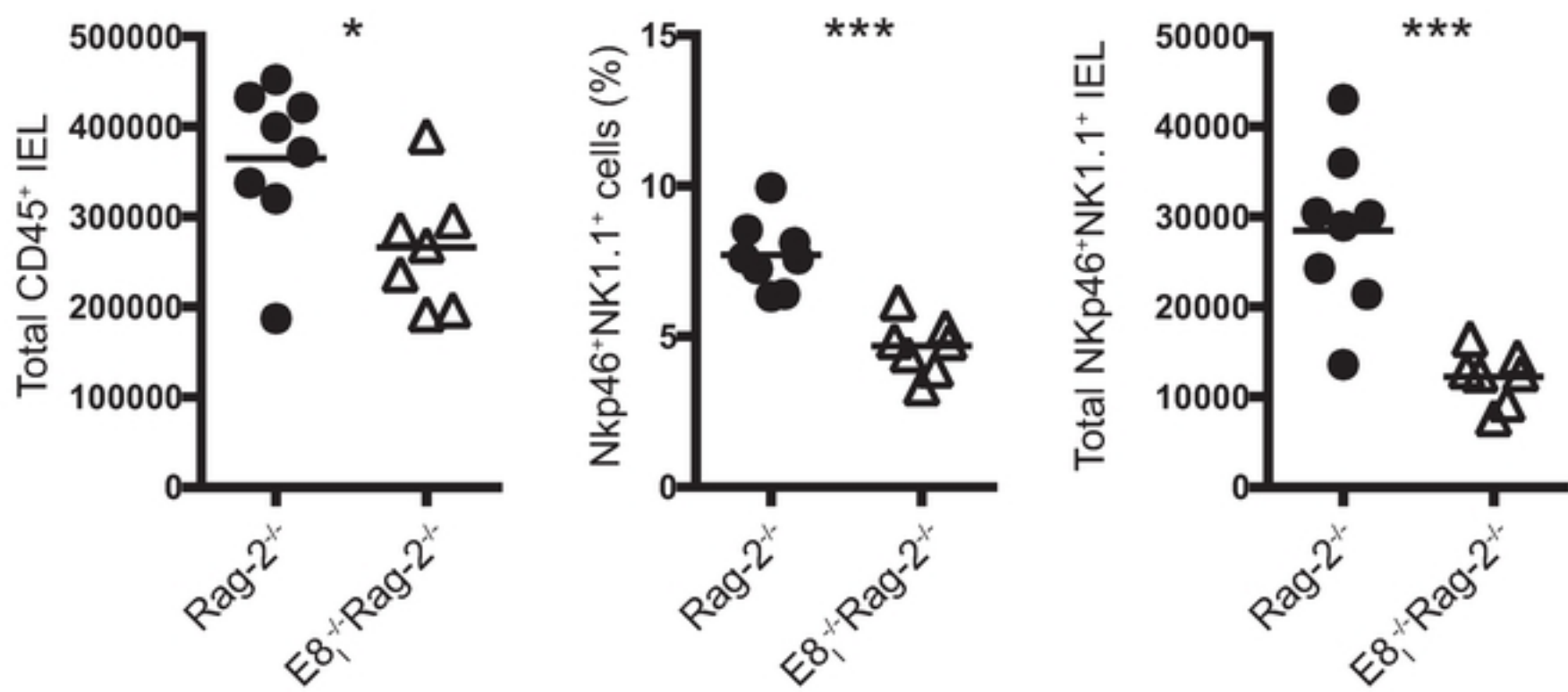
550 numbers in naïve Rag-2^{-/-} and Spp-1^{-/-}Rag-2^{-/-} mice; each symbol represents and individual
551 mouse (n=9 to 10). Data is representative of 3 experiments. * $p<0.05$, ** $p<0.01$ using two-way
552 ANOVA (a) or unpaired two-tailed Student's T test (b, c, d).

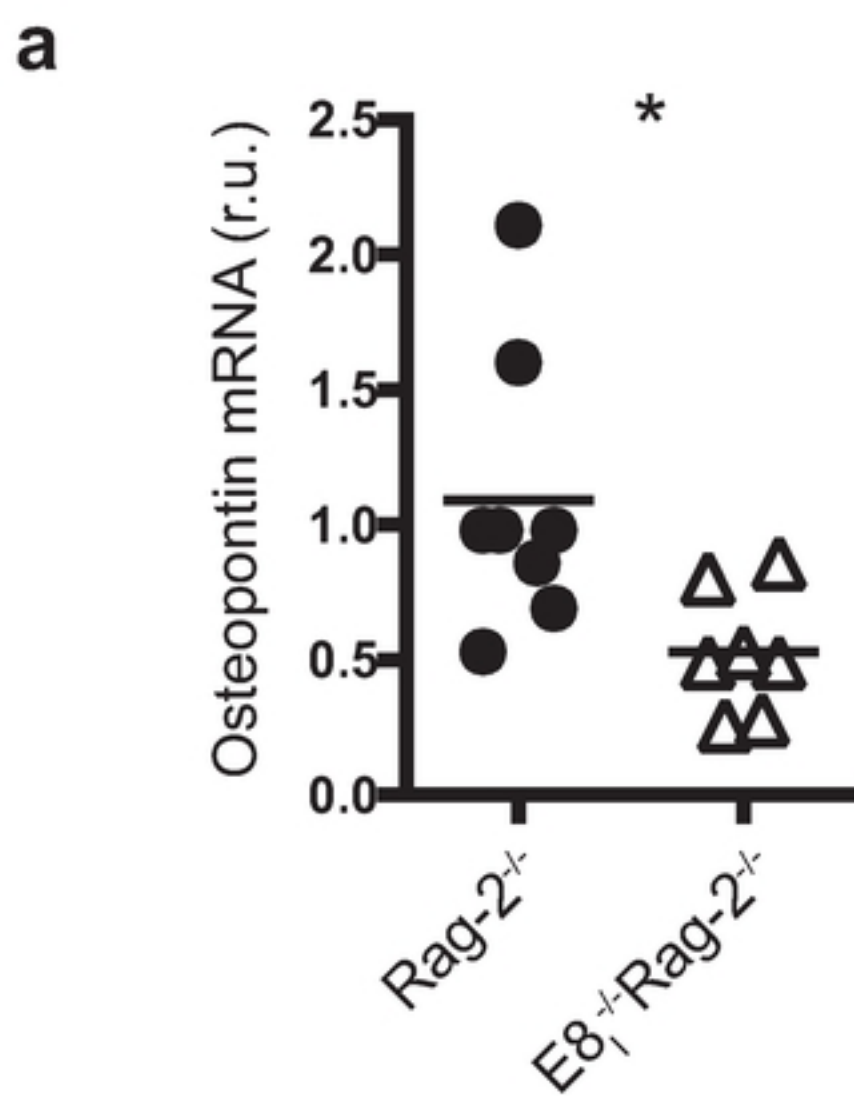
553

554 Fig. 6. *Decreased intestinal inflammation in mice deficient in iCD8 α cells.* Rag-2^{-/-} and E8_I^{-/-}
555 Rag-2^{-/-} mice were treated with anti-CD40 and monitored for 7 days for weight change (a). (b) At
556 the endpoint, colons were harvested for pathological analysis. (c) Osteopontin mRNA expression
557 from the colons of anti-CD40 treated Rag-2^{-/-} and E8_I^{-/-}Rag-2^{-/-} mice at the indicated time points.
558 Data is representative of at least two independent experiments (n=6 to 8). (d) E8_I^{-/-}Rag-2^{-/-} mice
559 were treated with recombinant osteopontin or PBS at day -2, -1 and 1 before and after disease
560 induction with 70 μ g of anti-CD40 antibodies, and their weights monitored for 7 days. (e) At the
561 endpoint, colons were harvested for pathological analysis. Data is representative of at least 3
562 independent experiments (n=6 to 7). Each symbol represents and individual mouse. * $p<0.05$,
563 ** $p<0.01$, *** $p<0.01$ using two-way ANOVA (a, d), unpaired two-tailed Student's T test (b, c)
564 or one-way ANOVA (e).

565

566

a**b****Figure 1****Figure 1**



b

bioRxiv preprint doi: <https://doi.org/10.1101/606616>; this version posted April 11, 2019. The copyright holder for this preprint (which was not certified by peer review) is the author/funder, who has granted bioRxiv a license to display the preprint in perpetuity. It is made available under aCC-BY 4.0 International license.

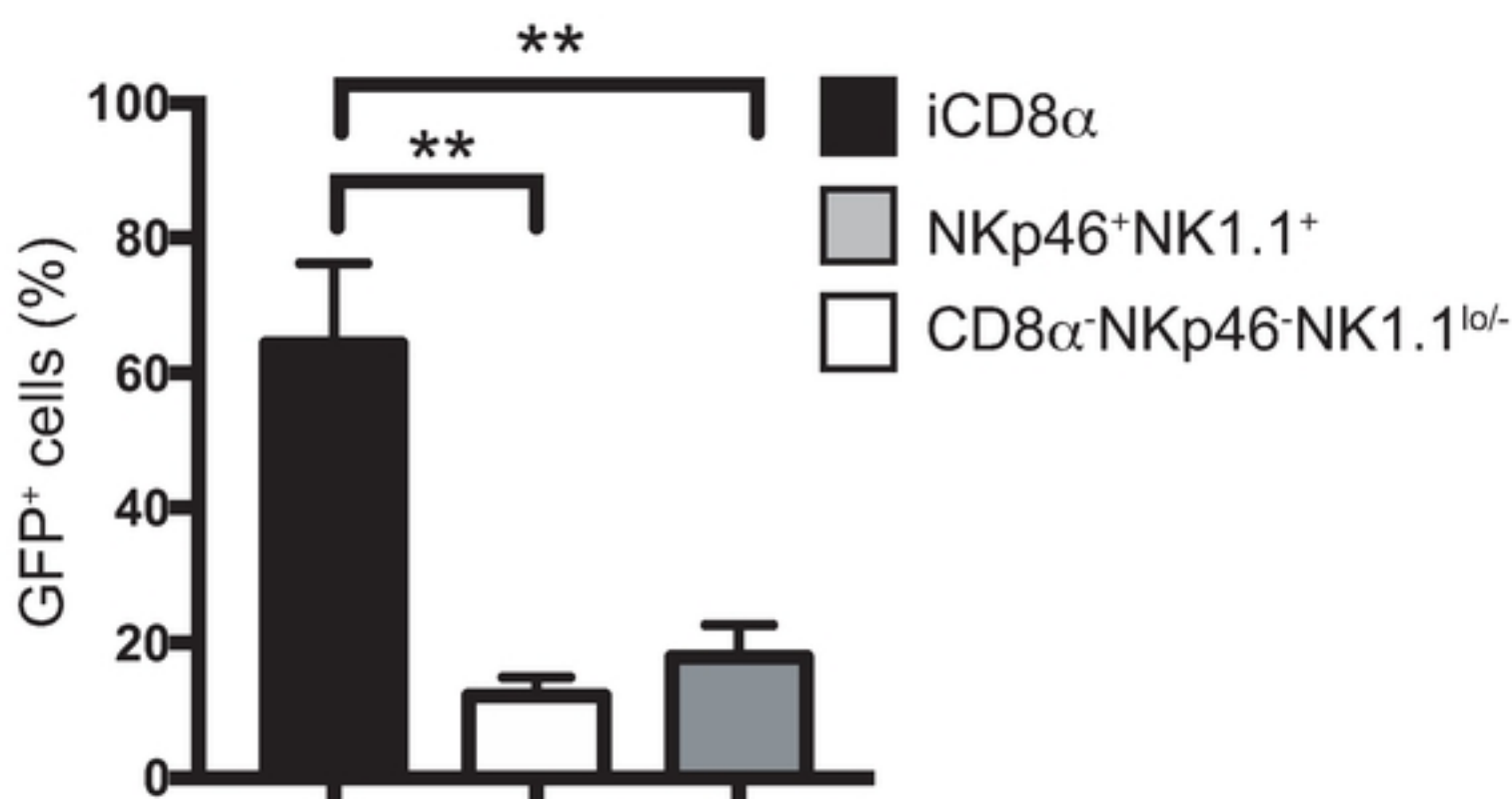
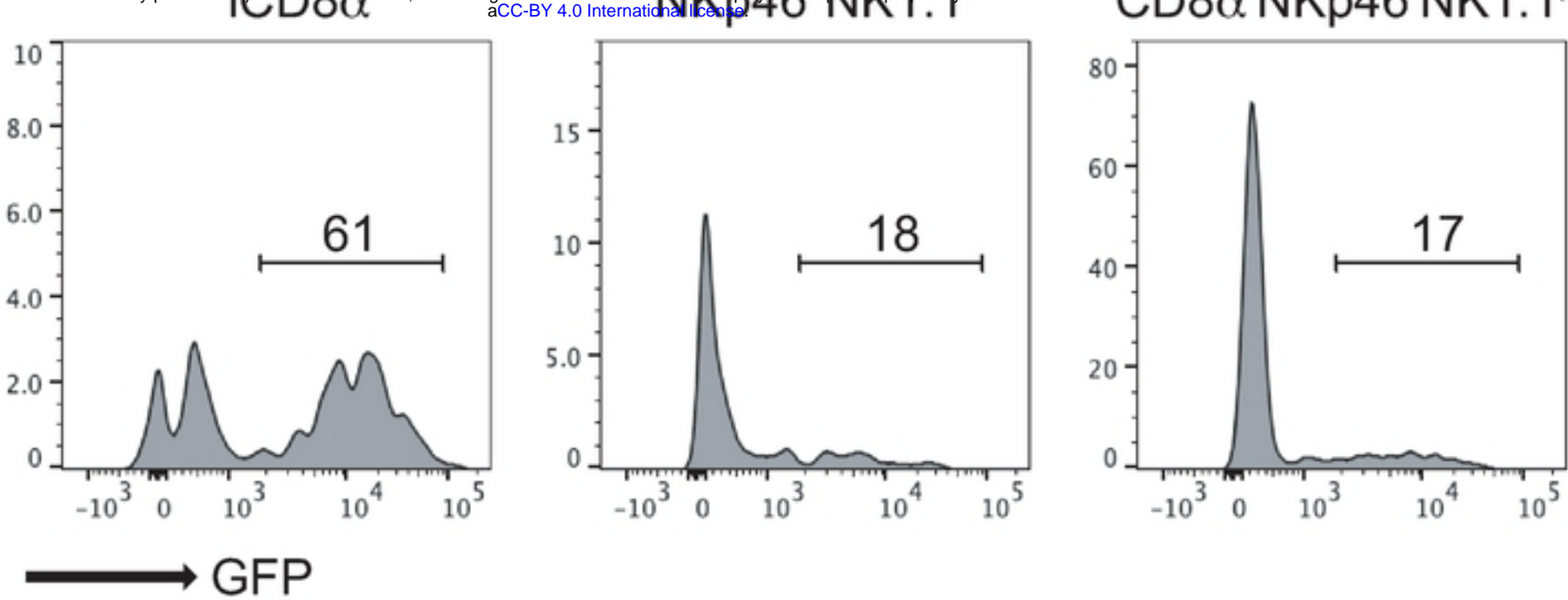
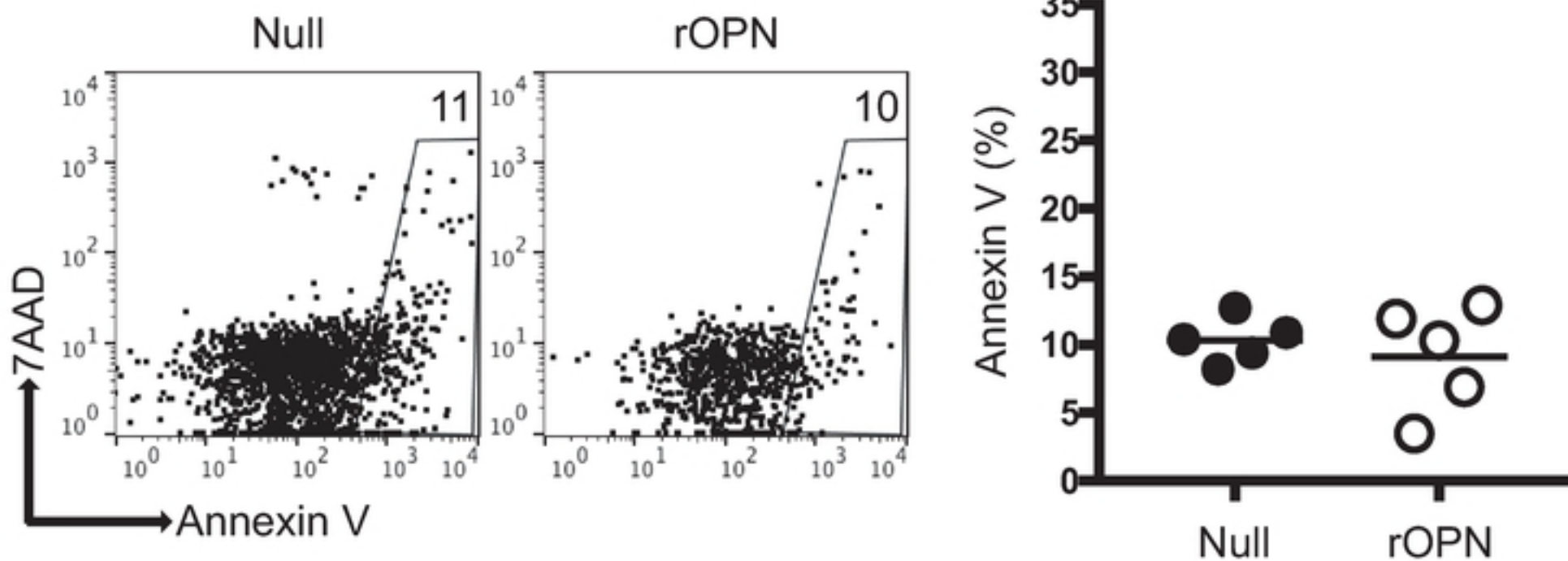
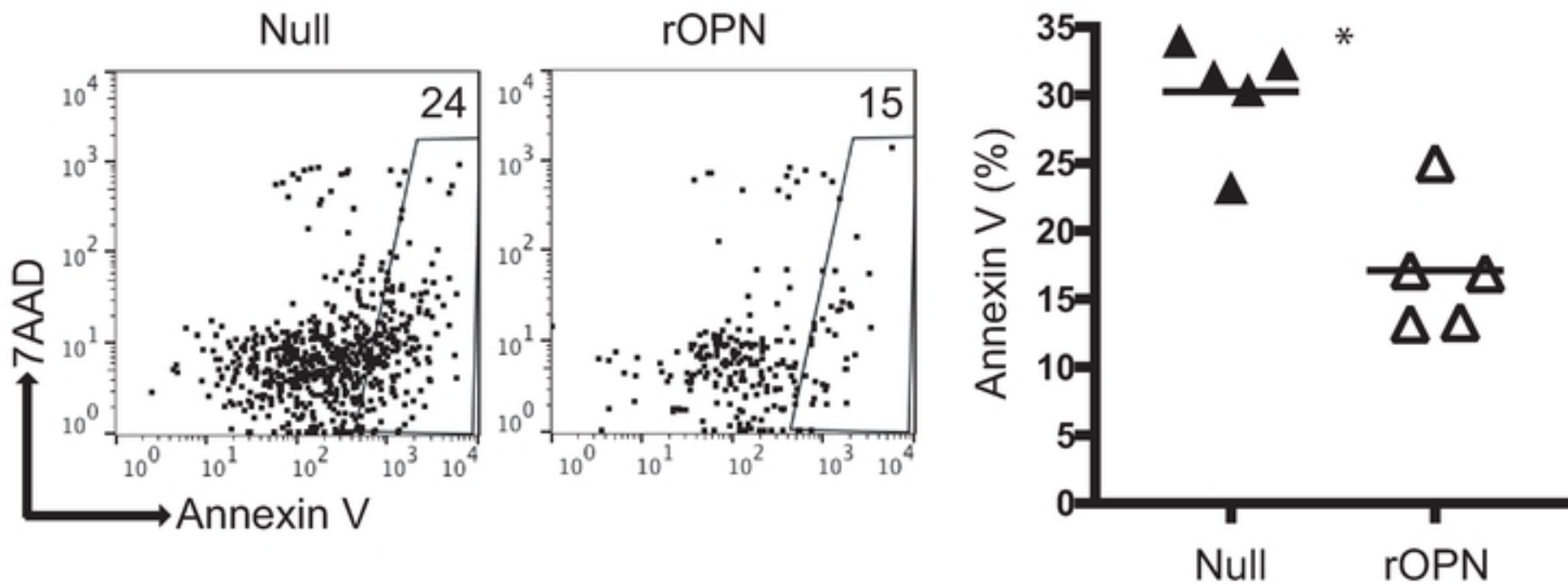
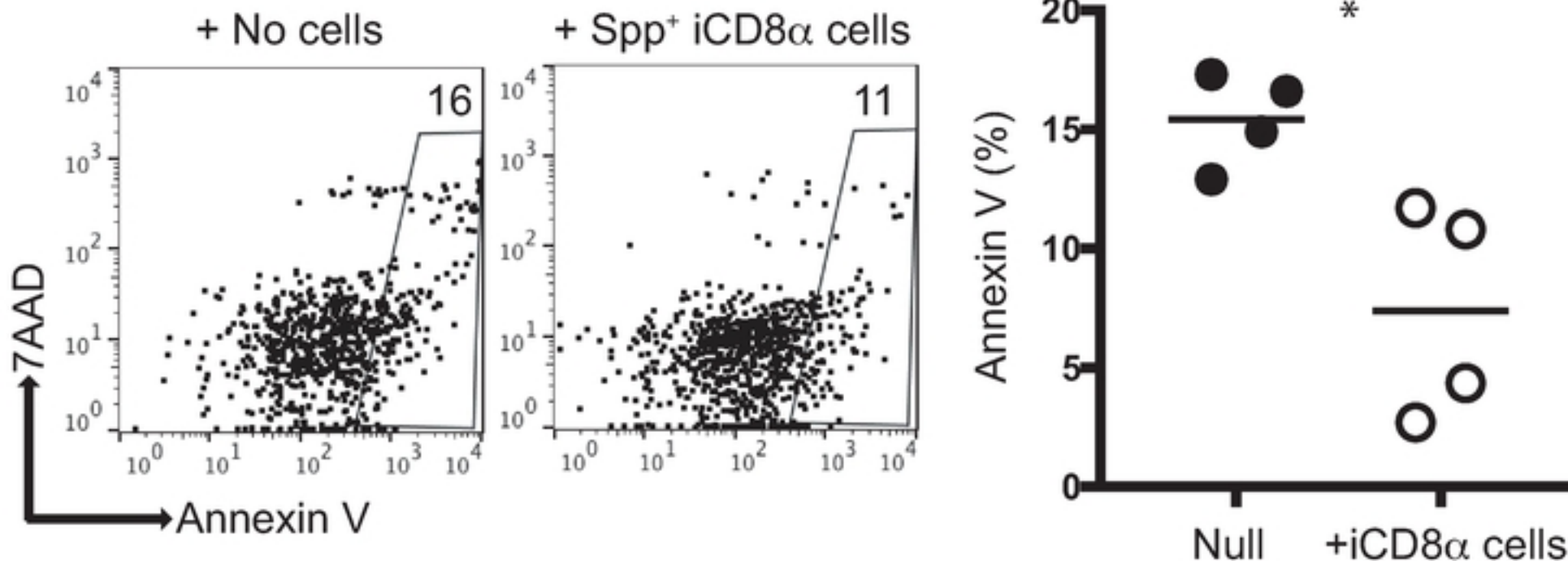


Figure 2

Figure 2

a**Rag-2^{-/-} CD45⁺ IEL**

bioRxiv preprint doi: <https://doi.org/10.1101/606616>; this version posted April 11, 2019. The copyright holder for this preprint (which was not certified by peer review) is the author/funder, who has granted bioRxiv a license to display the preprint in perpetuity. It is made available under aCC-BY 4.0 International license.

b**E8₁^{-/-} Rag-2^{-/-} CD45⁺ IEL****c****Spp-1^{-/-} Rag-2^{-/-} CD45⁺ IEL****Figure 3****Figure 3**

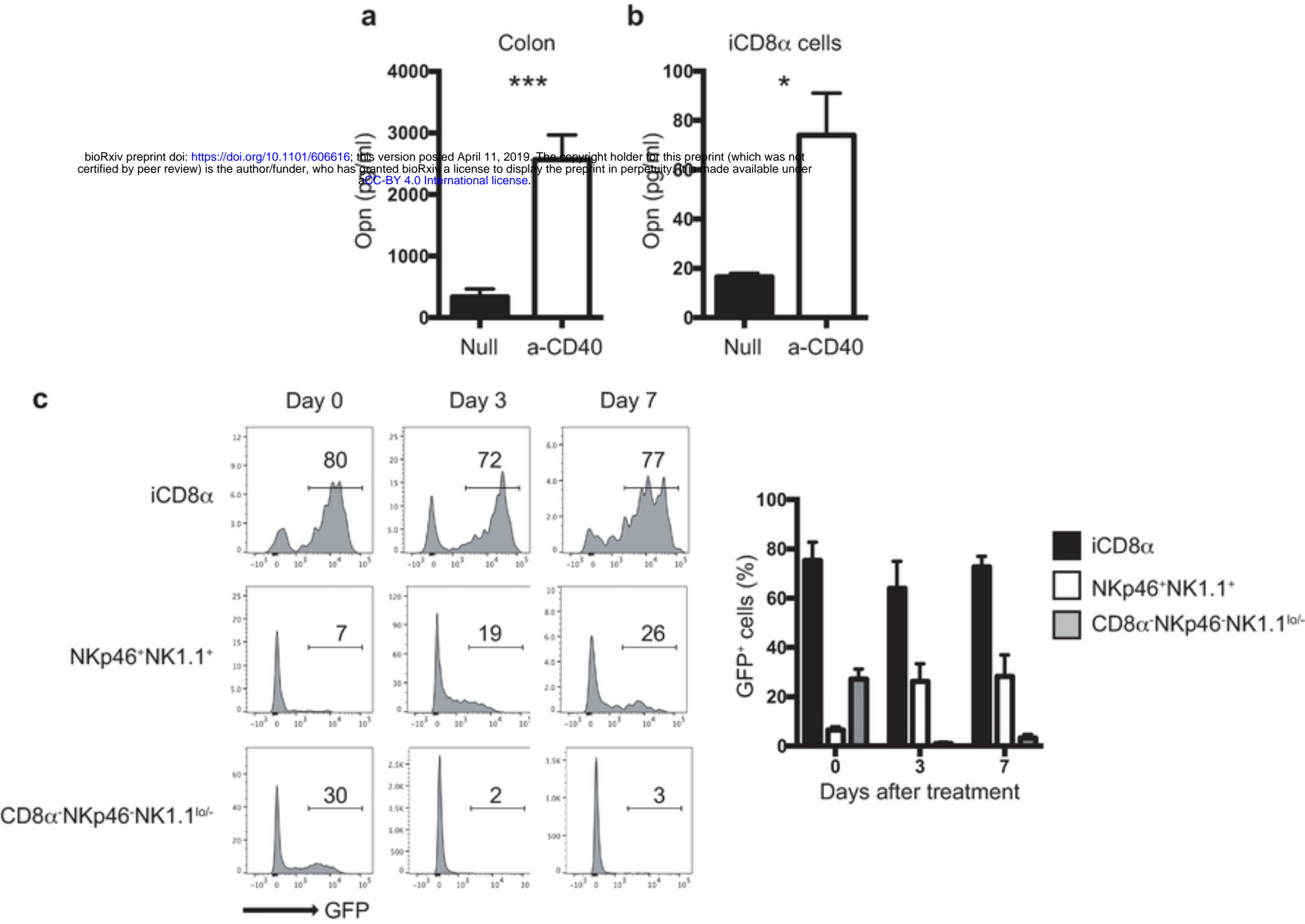


Figure 4

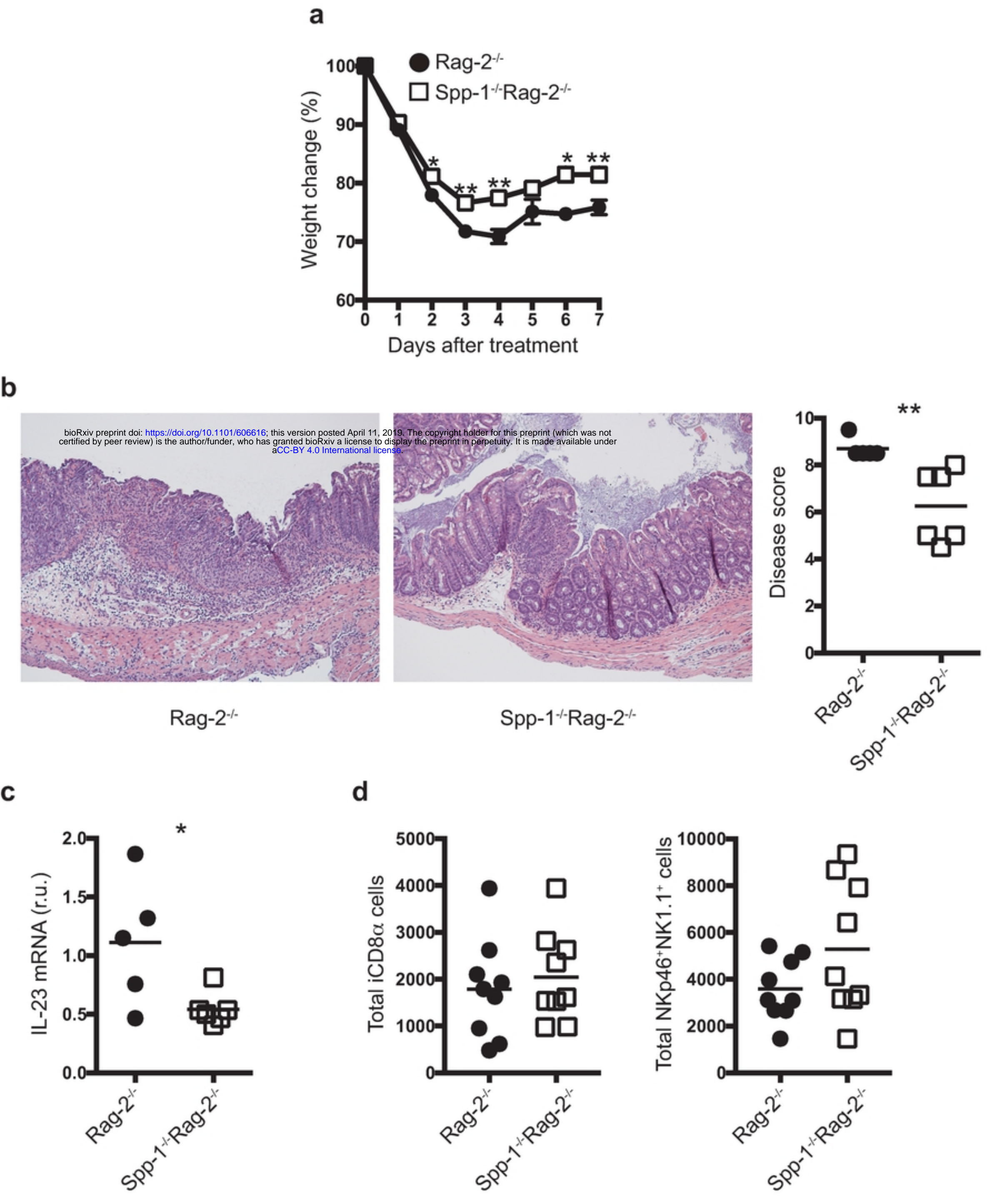


Figure 5

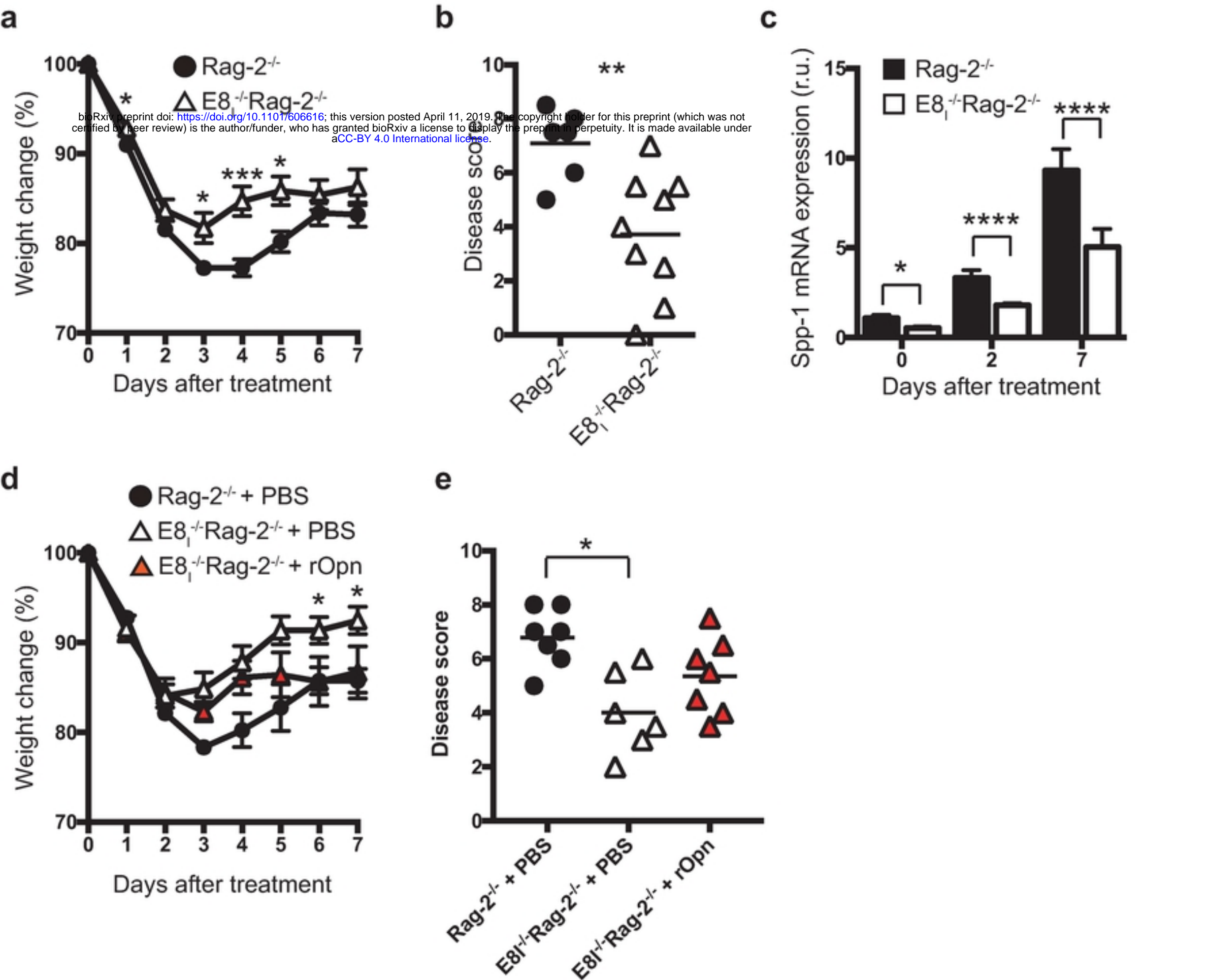


Figure 6

Figure 6